


Synthesis and Ionic Conductivity of Lithium Titanium Phosphate with NASICON-Type Structure Doping with Zirconium and Aluminum [†]

Anastasia Bocharova * and Irina Stenina 

Kurnakov Institute of General and Inorganic Chemistry, Russian Academy of Sciences, 31, Leninsky Prospekt, 119991 Moscow, Russia; stenina@igic.ras.ru

* Correspondence: ab.bocharova@mail.ru

[†] Presented at the 1st International Electronic Conference on Processes: Processes System Innovation, 17–31 May 2022; Available online: <https://ecp2022.sciforum.net>.

Abstract: In this work, new solid electrolytes $\text{Li}_{1+y}\text{Ti}_{2-x-y}\text{Zr}_x\text{Al}_y(\text{PO}_4)_3$ ($0 \leq x \leq 0.2$, $0 \leq y \leq 0.2$) were prepared by the sol-gel and solid-state methods (sintering temperatures: 800–1000 °C). The prepared materials were characterized by X-ray powder diffraction and scanning electron microscopy. Their conductivity was investigated by impedance spectroscopy in the temperature range of 25–200 °C. The activation energies of Li^+ transfer were calculated. The $\text{Li}_{1.2}\text{Ti}_{1.7}\text{Zr}_{0.1}\text{Al}_{0.2}(\text{PO}_4)_3$ material prepared by solid-state reaction exhibits the highest conductivity at 25 °C (6.2×10^{-4} S/cm).

Keywords: solid electrolyte; NASICON-type; lithium-ion conductor



Citation: Bocharova, A.; Stenina, I. Synthesis and Ionic Conductivity of Lithium Titanium Phosphate with NASICON-Type Structure Doping with Zirconium and Aluminum. *Eng. Proc.* **2022**, *19*, 16. <https://doi.org/10.3390/ECP2022-12617>

Academic Editor: Ioannis Spanopoulos

Published: 17 May 2022

Publisher's Note: MDPI stays neutral with regard to jurisdictional claims in published maps and institutional affiliations.



Copyright: © 2022 by the authors. Licensee MDPI, Basel, Switzerland. This article is an open access article distributed under the terms and conditions of the Creative Commons Attribution (CC BY) license (<https://creativecommons.org/licenses/by/4.0/>).

1. Introduction

Today, due to the growing demand for mobile power sources, lithium-ion batteries are becoming increasingly important because of their high power density and quite low self-discharge. However, there is still a problem with their application, caused by the flammability and insufficient electrochemical stability of the liquid electrolytes in most commercial batteries. In this regard, it is necessary to develop solid electrolytes with good stability and high ionic conductivity. Among all types of solid electrolytes with lithium conductivity, compounds with the NASICON-type structure are the most promising. However, a significant disadvantage of these materials is their insufficiently high ionic conductivity compared to liquid electrolytes. To increase the bulk conductivity, point defects can be created in their structure by isovalent (Zr^{4+}) and heterovalent (Al^{3+}) doping. This approach can significantly increase the bulk conductivity of lithium titanium phosphate by simultaneously changing the channel size and introducing additional Li^+ ions. In this work, $\text{Li}_{1+y}\text{Ti}_{2-x-y}\text{Zr}_x\text{Al}_y(\text{PO}_4)_3$ materials ($0 \leq x \leq 0.2$, $0 \leq y \leq 0.2$) were synthesized by both sol-gel (SG) and solid-state (SS) methods, by varying the final annealing temperature to determine the optimal synthesis method.

2. Methods

2.1. Materials and Reagents

The following raw materials were used for the synthesis of $\text{Li}_{1+y}\text{Ti}_{2-x-y}\text{Zr}_x\text{Al}_y(\text{PO}_4)_3$ ($0 \leq x \leq 0.2$, $0 \leq y \leq 0.2$): Li_2CO_3 (99%, Sigma-Aldrich, St. Louis, MI, USA), $(\text{C}_4\text{H}_9\text{O})_4\text{Ti}$ (99%, Alfa Aesar, Kandel, Germany) (or TiO_2 (98%, Chimmed, Moscow, Russia) in case of SS), $\text{NH}_4\text{H}_2\text{PO}_4$ (99%, Sigma-Aldrich, St. Louis, MI, USA), $(\text{C}_3\text{H}_7\text{O})_4\text{Zr}$ (70 wt.%, Sigma-Aldrich, St. Louis, MI, USA) (or $\text{Zr}(\text{HPO}_4)_2 \cdot 2\text{H}_2\text{O}$ (99.99%, Sigma-Aldrich, St. Louis, MI, USA) in case of SS) and $\text{Al}(\text{NO}_3)_3 \cdot 9\text{H}_2\text{O}$ (99.997%, Sigma-Aldrich, St. Louis, MI, USA).

2.2. Methods

In both synthesis methods, the initial reagents were mixed in a stoichiometric ratio. In the case of the sol-gel method, a water–ethanol mixture was used and citric acid was added as a chelating agent. Figures 1 and 2 show $\text{Li}_{1+y}\text{Ti}_{2-x-y}\text{Zr}_x\text{Al}_y(\text{PO}_4)_3$ synthesis by the sol-gel and solid-state methods, respectively.

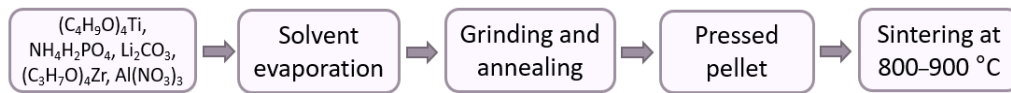


Figure 1. Scheme of synthesis of the $\text{Li}_{1+y}\text{Ti}_{2-x-y}\text{Zr}_x\text{Al}_y(\text{PO}_4)_3$ materials by sol-gel method.

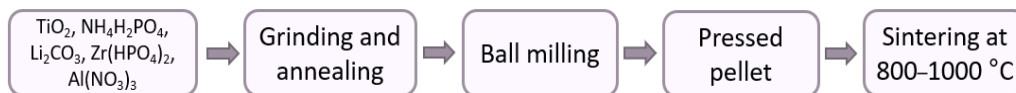


Figure 2. Scheme of synthesis of the $\text{Li}_{1+y}\text{Ti}_{2-x-y}\text{Zr}_x\text{Al}_y(\text{PO}_4)_3$ materials by solid-state method.

The X-ray diffraction (XRD) patterns were collected using Rigaku D/MAX 2200 (Cu K α radiation). The ion conductivity of the sintered pellets with silver electrodes was measured by impedance spectroscopy using an Elins Z1500 PRO impedance meter with an AC amplitude of 80 mV, from 10 Hz to 2×10^6 MHz, in the temperature range of 25–200 °C. Scanning electron microscopy (SEM) (Tescan Amber GMH (Kohoutovice, Czech Republic)) was used to analyze the morphology of the samples.

3. Results and Discussion

3.1. XRD

Figures 3 and 4 present the X-ray diffraction patterns of $\text{Li}_{1+y}\text{Ti}_{2-x-y}\text{Zr}_x\text{Al}_y(\text{PO}_4)_3$ ($0 \leq x \leq 0.2$, $0 \leq y \leq 0.2$) prepared by the sol-gel and solid-state methods.

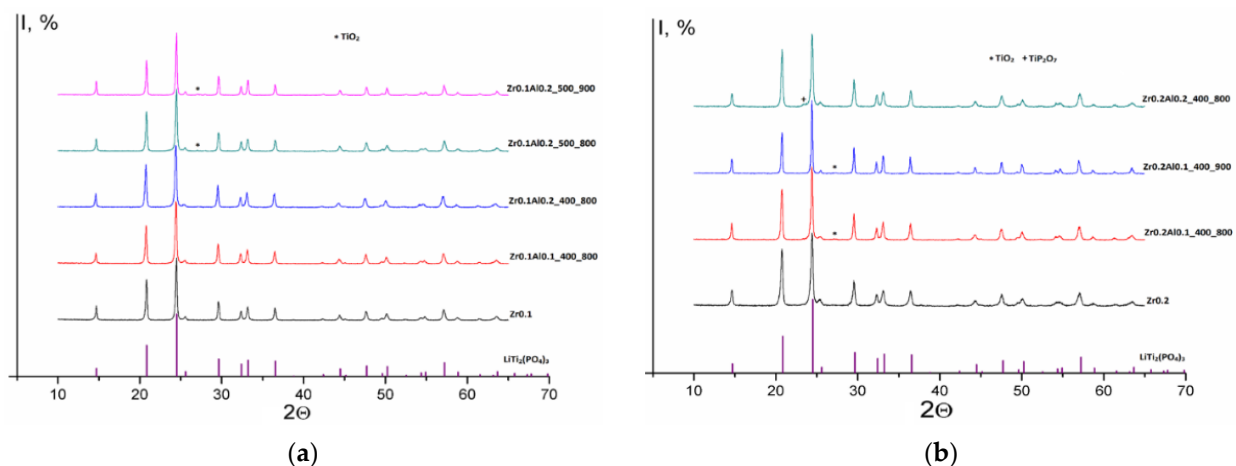


Figure 3. X-ray diffraction patterns of $\text{Li}_{1+y}\text{Ti}_{1.9-y}\text{Zr}_{0.1}\text{Al}_y(\text{PO}_4)_3$ (a) and $\text{Li}_{1+y}\text{Ti}_{1.8-y}\text{Zr}_{0.2}\text{Al}_y(\text{PO}_4)_3$ ($y = 0-0.2$) (b) prepared by sol-gel method.

The diffraction peaks are similar for all the samples and correspond to lithium titanium phosphate (PDF-2, card #35-0754). Some samples have TiO_2 , TiP_2O_7 and ZrP_2O_7 impurities, the presence of which can negatively affect the ionic conductivity.

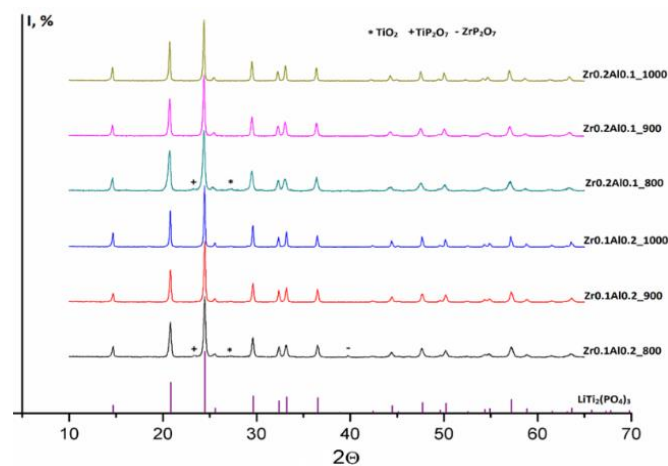
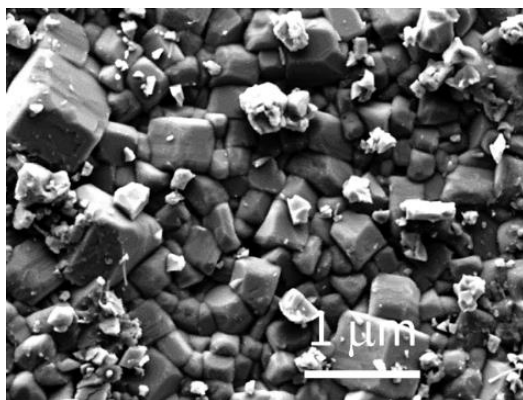


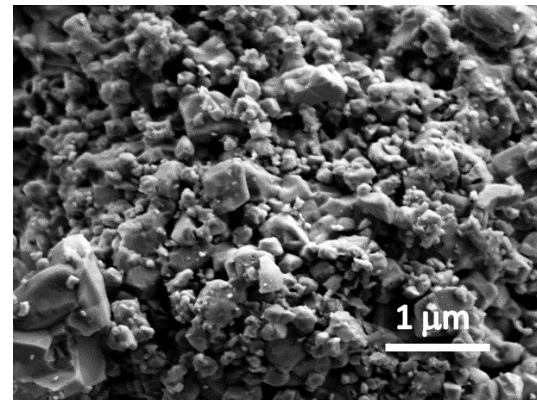
Figure 4. X-ray diffraction patterns of $\text{Li}_{1+y}\text{Ti}_{2-x-y}\text{Zr}_x\text{Al}_y(\text{PO}_4)_3$ ($x = 0\text{--}0.2$, $y = 0\text{--}0.2$) prepared by solid-state reaction.

3.2. SEM

Scanning electron microscopy images are shown in Figures 5 and 6.

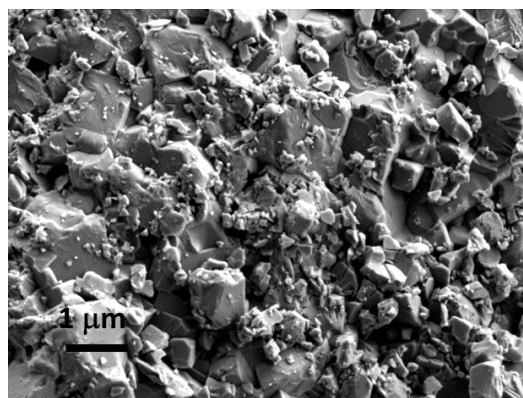


(a)

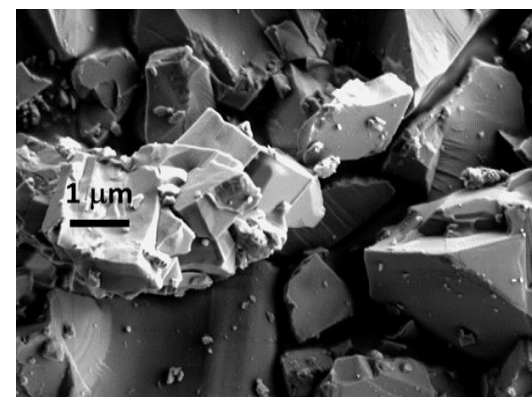


(b)

Figure 5. SEM images of $\text{Li}_{1.2}\text{Ti}_{1.7}\text{Zr}_{0.1}\text{Al}_{0.2}(\text{PO}_4)_3$ (a) and $\text{Li}_{1.2}\text{Ti}_{1.6}\text{Zr}_{0.2}\text{Al}_{0.2}(\text{PO}_4)_3$ (b) prepared by sol-gel method at 800 °C.



(a)



(b)

Figure 6. SEM images of $\text{Li}_{1.2}\text{Ti}_{1.7}\text{Zr}_{0.1}\text{Al}_{0.2}(\text{PO}_4)_3$ (a) and $\text{Li}_{1.2}\text{Ti}_{1.7}\text{Zr}_{0.1}\text{Al}_{0.2}(\text{PO}_4)_3$ (b) prepared by solid-state method at 900 °C and 1000 °C, respectively.

The SEM images demonstrate that the solid-state method results in more sintered ceramics with a larger particle size, which, in turn, agrees with the density of the produced ceramics. Thus, for samples prepared by the sol-gel method, the density is in the range of 1.87–2.28 g/cm³, while for materials prepared by the solid-state method, the ceramics density is in the range of 2.13–2.75 g/cm³.

3.3. Ionic Conductivity

The temperature dependences of ionic conductivity of the $\text{Li}_{1+y}\text{Ti}_{2-x-y}\text{Zr}_x\text{Al}_y(\text{PO}_4)_3$ ($0 \leq x \leq 0.2$, $0 \leq y \leq 0.2$) materials prepared by the sol-gel and solid-state methods are shown in Figures 7 and 8, respectively.

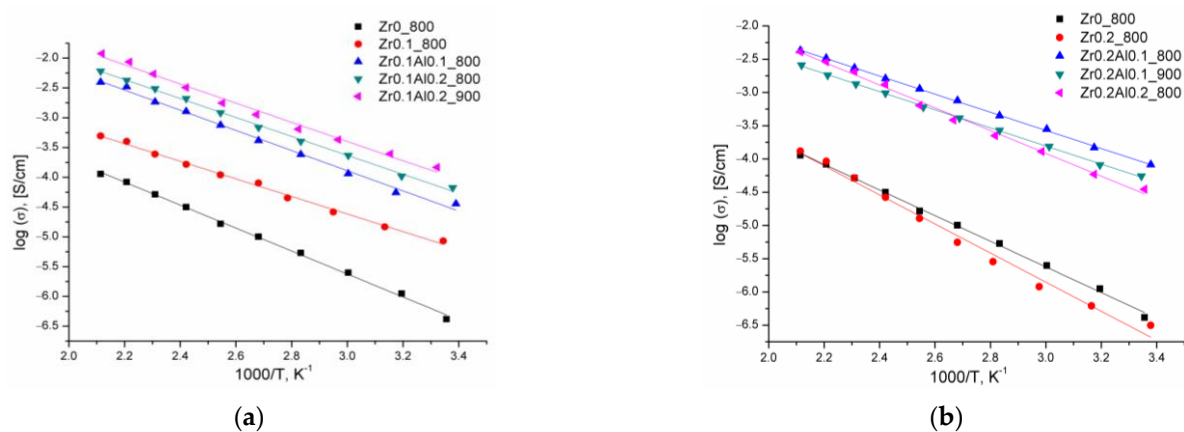


Figure 7. Plots of ionic conductivity vs. temperature of $\text{Li}_{1.2}\text{Ti}_{1.7}\text{Zr}_{0.1}\text{Al}_{0.2}(\text{PO}_4)_3$ (a) and $\text{Li}_{1.2}\text{Ti}_{1.6}\text{Zr}_{0.2}\text{Al}_{0.2}(\text{PO}_4)_3$ (b) prepared by sol-gel method.

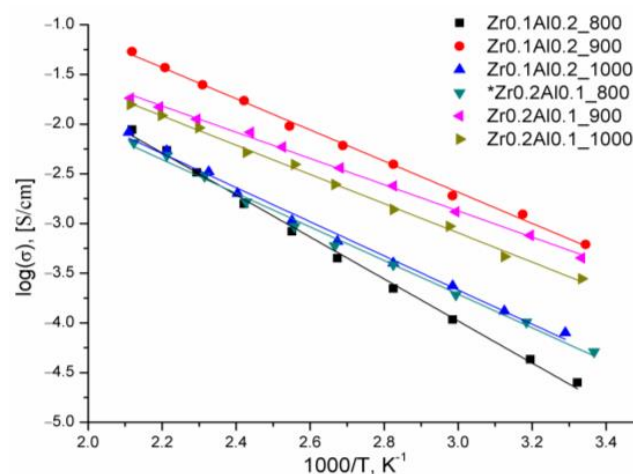


Figure 8. Plots of ionic conductivity vs. temperature of $\text{Li}_{1+y}\text{Ti}_{2-x-y}\text{Zr}_x\text{Al}_y(\text{PO}_4)_3$, $x = 0-0.2$, $y = 0-0.2$, prepared by solid-state method.

Ion conductivity increases significantly with the substitution of 5% titanium by zirconium in $\text{LiTi}_2(\text{PO}_4)_3$. Increasing the zirconium content has the opposite effect, and the conductivity of the resulting material becomes like that of the pristine lithium titanium phosphate. A similar effect was reported elsewhere [1,2]. In all cases, the additional introduction of aluminum leads to an increase in conductivity. The optimal composition with the highest lithium conductivity was determined ($\text{Li}_{1.2}\text{Ti}_{1.7}\text{Zr}_{0.1}\text{Al}_{0.2}(\text{PO}_4)_3$)— 6.2×10^{-4} at 25 °C). The activation energies of conductivity of the obtained materials are in the range of 30–49 kJ/mol.

Author Contributions: Conceptualization, I.S. and A.B.; methodology, I.S.; investigation, A.B. and I.S.; data curation, I.S.; writing—original draft preparation, A.B.; writing—review and editing, I.S.; supervision, I.S.; project administration, I.S. All authors have read and agreed to the published version of the manuscript.

Funding: This work was supported by the Ministry of Science and Higher Education of the Russian Federation as part of the State Assignment of the Kurnakov Institute of General and Inorganic Chemistry of the Russian Academy of Sciences.

Institutional Review Board Statement: Not applicable.

Informed Consent Statement: Not applicable.

Data Availability Statement: The data presented in this study are available on request from the corresponding author.

Conflicts of Interest: The authors declare no conflict of interest.

References

1. Rai, K.; Kundu, S. Fabrication and performances of high lithium-ion conducting solid electrolytes based on NASICON $\text{Li}_{1.3}\text{Al}_{0.3}\text{Ti}_{1.7-x}\text{Zr}_x(\text{PO}_4)_3$ ($0 \leq x \leq 0.2$). *Ceram. Int.* **2020**, *46*, 23695–23705. [[CrossRef](#)]
2. Rao, A.V.; Veeraiah, V.; Rao, A.V.; Babu, B.K.; Kumar, K.V. Influence of Zr^{4+} doping on structural, spectroscopic and conductivity studies of lithium titanium phosphate. *Ceram. Int.* **2014**, *40*, 13911–13916.